Food Chemistry 408 (2023) 135232

Contents lists available at ScienceDirect

Food Chemistry

journal homepage: www.elsevier.com/locate/foodchem

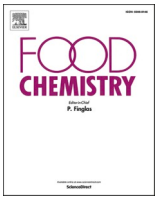

Integrated metabolomics analysis of *Lactobacillus* in fermented milk with fish gelatin hydrolysate in different degrees of hydrolysis

Yi Le [a], Xiaowei Lou [a,b], Chengwei Yu [a,c], Chenxi Guo [a], Yun He [a,b], Yuyun Lu [a], Hongshun Yang [a,b,*]

[a] Department of Food Science and Technology, National University of Singapore, 117542, Singapore
[b] National University of Singapore (Suzhou) Research Institute, 377 Lin Quan Street, Suzhou Industrial Park, Suzhou, Jiangsu 215123, China
[c] School of Health, Jiangxi Normal University, Nanchang, Jiangxi 330022, China

ARTICLE INFO

Keywords:
Fish gelatin hydrolysate
Lactobacillus
Integrated metabolomics
NMR
UPLC-MS
Fermented milk
Foodomics

ABSTRACT

Dual-platform metabolomics combined with multivariate data analysis was used to investigate the effects of adding fish gelatin (FGH) at different degrees of hydrolysis (DH) on the growth and metabolic pathways of different species of *Lactobacillus* in fermented milk. The results showed that the promotion effect of FGH on *Lactobacillus* was related to the species of probiotics. The corresponding metabolic pathways also changed, with the promotion of *Lactobacillus* by FGH mainly regulated through amino acid metabolism, lipid metabolism, and nucleotide metabolism pathways. The excess DH inhibited the growth of *L. paracasei* by adjusting its metabolic state through reducing nucleotide requirements, allocating protein resources, and adopting a stress response. In conclusion, this study revealed the effectiveness of dual-platform metabolomics in explaining the metabolic mechanisms of probiotics, providing theoretical support and a scientific basis for the development of functional fermented foods.

1. Introduction

It is common for fermented dairy products to be prepared with single probiotics, such as Yakult, LAJOIE, and Cherita. An essential requirement for these products is that probiotic must be present in sufficient numbers in the fermented product to benefit the human body. Most of these single probiotics belong to the genus *Lactobacillus*. However, slow growth and low survival are critical problems in single probiotic fermented milk. This dilemma is attributed to the lack of specific nutritional factors in milk. Besides, some *Lactobacillus* cannot synthesize amino acids and cell envelope protease (CEP), which limits its rapid propagation (Li et al., 2020).

The peptides are better absorbed by probiotics than amino acids at the same concentration. Further enzymatic digestion of fish gelatin (FG) yields a product called fish gelatin hydrolysate (FGH), which contains peptides consisting of two or more amino acid units joined by a peptide bond. A previous study has shown that protein hydrolysates from poultry waste sources can effectively promote the growth of probiotics (Lazzi et al., 2013). Whereas in most studies, peptide promoted probiotics were carried out on cultural media. This growth condition is ideal for the growth of the target microorganisms but cannot reproduce the conditions in practical application scenarios. It is also worth noting that the degree of hydrolysis (DH) of FGH dramatically affects the length of the peptide chain and the degree of exposure of the terminal amino group (Alemán et al., 2011). Higher DH corresponds to a higher number of peptides in general. Therefore, it is also essential to study what level of hydrolysis is most suitable for the growth of probiotics. However, the current understanding of the basic mechanisms of probiotic growth-promoting processes is minimal and the application of different levels of hydrolyzed FGH in milk matrices to improve the quality of fermented milk has not been investigated.

Metabolomics can comprehensively and systematically reveal changes in bacterial intracellular metabolism following the addition of variable external supplements (Guo et al., 2022). Nuclear magnetic

Abbreviations: NMR, nuclear magnetic resonance; UPLC-MS, ultra-high performance liquid chromatography-mass spectrometry; LA-5, *Lactobacillus acidophilus* LA-5; L431, *Lacticaseibacillus paracasei* subsp. *paracasei* CASEI 431; FGH, fish gelatin hydrolysate; DH, degrees of hydrolysis; CEP, cell envelope protease; FG, fish gelatin; MRS, Deman-Rogasa; PBS, phosphate-buffered saline; TVC, total viable count; DI, deionized; TSP, Trimethylsilyl propionic acid; VIP, variable importance in projection; FC, fold change; PCA, principal component analysis; PC, principal component; OPLS-DA, orthogonal projection to potential structure discriminant analysis.

* Corresponding author at: Department of Food Science and Technology, National University of Singapore, 117542, Singapore.
E-mail address: hongshunyang@hotmail.com (H. Yang).

https://doi.org/10.1016/j.foodchem.2022.135232
Received 4 October 2022; Received in revised form 12 December 2022; Accepted 14 December 2022
Available online 17 December 2022

resonance (NMR) spectroscopy and ultra-performance liquid chromatography-mass spectrometry (UPLC-MS) are two major metabonomic techniques in practical use. The former has the advantage of being reproducible and non-destructive to the sample (Emwas, 2015), while the latter has the advantage of being able to combine the high resolution of chromatography with the high sensitivity of mass spectrometry and is used for the analysis of sub-biological samples (Ashraf et al., 2020). Given the respective advantages of these two techniques, NMR and UPLC-MS were combined to provide a comprehensive understanding of the growth-promoting process and metabolic response of *Lactobacillus* in fermented milk to the addition of FGH with different DH.

This study aimed to determine the mechanisms of promotion and metabolic effects of different DH of FGH on *Lactobacillus*. The strains were *Lacticaseibacillus paracasei* subsp. *paracasei* CASEI 431 (L431) and *Lactobacillus acidophilus* LA-5 (LA-5), which are now widely used in various probiotic fermented milk due to their own potential health benefits (Corona-Hernandez et al., 2013). Fish gelatin at 5 %, 10 %, 15 %, and 20 % hydrolysis degree was added to the fermented milk, respectively. In addition, the mechanism of the effect of hydrolysate on probiotics was further investigated through microbiological analysis and untargeted dual platform metabolomics combined with multivariate data analysis.

2. Materials and methods

2.1. Materials

L431 and LA-5 were supplied from Chr. Hansen Co. ltd (Singapore). Skim milk powder was purchased from Nature ltd. (Singapore). FG (200 Bloom) was purchased from Chengdu Jingdian Co. ltd. (Sichuan, China). Methanol-d_4 was purchased from Cambridge Isotope Laboratories (Miami, FL, USA). LC-MS grade methanol was purchased from Waters (Milford, MA, USA). Pancreatin from porcine pancreas (EC: 232. 468. 9; 96.7 U/mL based on trypsin activity) and other chemicals (analytical grade) were purchased from Sigma-Aldrich Co. ltd (Singapore).

2.2. Hydrolysis of fish gelatin

FG (3 g) was dissolved in 80 mL of distilled water. After adjusting it to pH 8 by 0.05 mol/L sodium hydroxide, the distilled water was then increased to 100 mL to obtain a final concentration of 3 % (w/v). The hydrolysis reaction was started by the addition of pancreatin at various amounts as described by Benjakul and Morrissey (1997) to obtain DH of 5 %, 10 %, 15 % and 20 %, respectively. The hydrolysis reaction was carried out at 50 °C for 4 h, followed by heating at 90 °C for 15 min to deactivate it. The resulting mixture was then centrifuged for 10 min (25 °C, 5000 × *g*). The supernatant was collected and then freeze-dried (Lyovapor™ L-300, Buchi, Switzerland) to obtain FGH, which was placed in polyethylene bags and stored at −20 °C for subsequent experiments.

The DH of FGH was determined using formaldehyde titration. For 2 g of sample, 70 mL of water was added in a beaker placed on a magnetic stirrer. The pH of the solution was adjusted to 8.2 by 0.05 mol/L sodium hydroxide before 10 mL of formaldehyde (37 wt% in H_2O) was added to the solution. Titration was then carried out with 0.05 mol/L sodium hydroxide until the pH of the sample reached 9.20 using a pH meter (Thermo Orion pH meter, Waltham, MA, USA). Free amino groups were determined by formol titration and total nitrogen was determined according to the Dumas combustion method (Jung et al., 2003). DH was calculated according to the following equation:

DH = [% Free amino groups/% total nitrogen] × 100.

2.3. Bacterial strains and culture conditions

Lyophilized *Lactobacillus acidophilus* LA-5 and *Lacticaseibacillus paracasei* subsp. *paracasei* CASEI 431 were inoculated onto Deman-Rogasa (MRS) broth (Merck) and incubated under anaerobic and aerobic conditions (37 °C, 24 h), respectively. A second succession of cultures was prepared and cultured (37 °C, 48 h) in the same way. Bacterial precipitates were collected by centrifugation (10,000 × *g*, 10 min, 4 °C) and washed twice with 0.1 mol/L phosphate-buffered saline (PBS, pH 7.2) and resuspended (Ozturkoglu-Budak et al., 2019).

2.4. Preparation of fermented milk

The preparation of fermented milk was shown in Fig. S1. According to the previous study in our group, the FGH with DH of 0 % (FGH-0) was added at 0.4 % (w/w) to reconstituted skim milk (total solids 10 g/100 g) as the control group (Yin et al., 2021). FGH with DHs of 5 % (FGH-5), 10 % (FGH-10), 15 % (FGH-15), and 20 % (FGH-20) was added separately to reconstituted skim milk (total solids 10 g/100 g) at the amount yielding an equivalent level of nitrogen content to FGH-0 determined by Dumas combustion method (Jung et al., 2003). The mixture of skim milk and FGH with different DHs were was then heated to 121 °C (5 min) under high pressure, followed by immediate cooling to 42 °C and inoculation with LA-5 or L431 (approximately 10^8 CFU/mL). Subsequently, the milk was put into an incubator (42 °C) for 20 h. The fermented milk was then removed from the incubator and rapidly cooled and stored at 4 °C for 48 h for post-fermentation.

2.5. Enumeration of total viable cells (TVC)

TVC was counted by spread plate technique with some modifications (Faraki et al., 2020). Before and after fermentation, 10 mL of fermented milk samples with different strains were mixed with 90 mL of deionized (DI) water in a stomach bag and then homogenized for 2 min to mix well. Subsequently, tenfold serial dilutions in 0.1 % (w/v) buffered peptone water were used and incubated in MRS agar. LA-5 and L431 were incubated under anaerobic and aerobic conditions for 72 h (37 °C), respectively.

2.6. Extraction and preparation of probiotics metabolites

Fermented milk (30 mL) containing bacterial cells was diluted with 0.1 % peptone water (270 mL). Diluted samples were centrifuged at 500 × *g* for 2 min at 4 °C to precipitate cells (Wang, Zhou, & Yang, 2022). Afterward, the cells suspension obtained by low-speed centrifugation was washed twice with 5 mL PBS and re-centrifuged (12,000 × *g*, 10 min, 4 °C). The pellets were resuspended with about 1 mL of cold methanol-d_4 solution for NMR or ice-cold (MS grade) methanol for UPLC-MS analysis. Cells were completely lysed by three freeze–thaw cycles in liquid nitrogen to extract intracellular metabolites, and metabolites were centrifuged to collect (12,000 × *g*, 20 min, 4 °C). For NMR analysis, Trimethylsilyl propionic acid (TSP) (1 mmol/L) was dissolved in methanol-d_4 in advance. Then, TSP as an internal standard was transferred to the NMR tube to determine the concentration of individual metabolites. For UPLC-MS analysis, 0.1 mmol/L gallic acid as an internal standard was added before being injected through a sterile nylon 0.2 μm filter into the HPLC vial (Wang, Gao, & Yang, 2022).

2.7. UPLC/Q-TOF-MS measurement

Metabolomics analysis was performed with an ACQUITY UPLC™ I-Class PLUS system (Waters, Milford, MA, USA) equipped with a VION ion mobility spectroscopy quadrupole time-of-flight mass spectrometer (IMS-QTOF-MS) (Waters, Manchester, U.K.). An Acquity HSS T3 column was selected (1.8 μm, 2.1 * 30 mm; Waters, Manchester, UK) with a column oven temperature of 30 °C, and the temperature of auto-sampler was maintained at 8 °C. The mobile phases were 0.1 % formic acid in water (A) and acetonitrile (B), all used solutions were LC-MS grade. The linear gradient program began with 1 % B for 1.5 min; 1.5–8 min increases in B from 1 % to 70 %; 8–13 min increases in B from 70 % to 90

%; 13–13.5 min increase in B from 90 % to 99 %; 13.5–16 min held at 99 % B; and 16–20 min (post-acquisition time) starting mobile phase 1 % B to re-equilibrate the column. The mobile phase injection volume was 5 μL and the flow rate was 300 μL/mL. ionization was performed in ESI- and ESI + modes. The mass range was set to *m/z* 50–800 Da and the scan time was 0.2 s. The ESI source conditions were as follows: capillary voltages, 1.8 kV (ESI +) and 2.3 kV (ESI −) for LA-5, as well as 6.13 kV (ESI +) and 2.5 kV (ESI−) for L431, were used for the detection of probiotic metabolites; The source temperature and desolvation temperature are 120 °C and 500 °C, respectively. Nitrogen was used as desolvation and cone gas with a flow rate of 800 L/h.

2.8. NMR spectroscopic analysis

A Bruker DRX-500 NMR spectrometer with a ^{1}H resonance frequency of 500.23 MHz (Bruker, Rheinstetten, Germany) was used for metabolic analysis. The standard NOESY pulse sequence was used to gain the ^{1}H spectra of each sample with a width of 10 ppm. The spectrum was gained using 128 scans, and a 2 s relaxation delay. The free induction decays were multiplied using an exponential function equivalent to a 1-Hz line-broadening factor prior to Fourier transformation. 2D NMR spectra ^{1}H–^{13}C heteronuclear single quantum correlation (HSQC) was used for the confirmation of chemical signals of metabolites. In particular, the ^{1}H spectrum was acquired in the F2 channel with a spectral width of 10 ppm while the ^{13}C spectrum was tested in the F1 channel with a spectral width of 175 ppm (Wang, Zhou, & Yang, 2022).

2.9. Data processing

The NMR spectra were processed manually by Topspin 4.0.9 (Bruker) software, and the obtained spectral phases and baselines were manually corrected with reference to the chemical shifts of the TSP. The metabolites corresponding to the spectra were identified by referring to the NMR database and related studies. The databases were as follow: Madison Metabolomics Consortium Database (https://mmcd.nmrfam.wisc.edu/), and Human Metabolome Database (https://www.hmdb.ca/). Subsequently, the data were further processed and analyzed using SIMCA software (version 13.0, Umetrics, Umeå, Sweden), and the full region excluding 3.29–3.35 ppm containing the methanol signal was normalized to a width of 0.02 ppm. Principal component analysis (PCA) and orthogonal projection to potential structure discriminant analysis (OPLS-DA) were used for grouping to determine differences due to different treatments. The significant altered metabolites was selected by variable importance in projection (VIP) > 1, Fold change (FC) value > 2 and $P < 0.05$ (Wang, Gao, et al., 2022).

Progenesis QI software (V.2.4, Nonlinear Dynamics, Waters, Newcastle, U.K.) was used for the processing of UPLC-MS spectra. Peak picking, filtering, retention time alignment, and response normalization were performed automatically. The adducts $[M+H]^+$, $[M+NH_4]^+$, $[M+Na]^+$ and $[M+K]^+$ were selected in ESI+, and $[M-H]^-$ and $[M-H_2O-H]^-$ were selected in ESI- for metabolite identification, while the Kyoto Encyclopedia of Genes and Genomes (KEGG) database (https://www.genome.jp/kegg/pathway.html) and the HMDB were jointly used for reference. EZinfo (V.3.0, Umetrics, Sweden) was applied for PCA and OPLS-DA. Metabolites that were significantly changed in each FGH-added sample compared to the control were screened according to VIP > 1, $P < 0.05$ and CV ≤ 30 (Wang, Gao, et al., 2022). These data were combined with data obtained from NMR analysis to explain the main metabolic disturbances in *Lactobacillus* strains following the addition of FGH.

2.10. Statistical analysis

All experiments were repeated independently in triplicate. Statistical analysis of the obtained metabolite contents was performed using the one-way ANOVA (Duncan's Multiple Range Test) model in SAS 8.0 with a significant difference level of $P < 0.05$.

3. Results and discussions

3.1. The growth of Lactobacillus after adding FGH with different DH

The addition of FGH did promote the growth of probiotics significantly. As shown in Fig. 1, the growth of LA-5 was promoted notably after the addition of FGH with DHs of 10 %, 15 % and 20 %, respectively. The cell increments increased from 1.81 to 1.97 log CFU/L ($P < 0.05$) with the increase of DH (from 10 % to 20 %), whereas the control group only increased to 1.55 log CFU/L. As for L431, it was promoted significantly when the DH of FGH was less than or equal to 10 %. The growth amount increased from 1.79 log CFU/L in the control group to 2.12 log CFU/L in the FGH-10 group ($P < 0.05$). However, when DH was 15 %, the increment of probiotics was not considerably different from those in the control group. When DH further increased to 20 %, the growth of probiotics was decreased (reduced to 1.59 log CFU/L, $P < 0.05$). The FGH in larger DH, usually with a smaller molecular weight, would be easily absorbed and utilized by organisms. The promoting trend of LA-5 was consistent with this assumption. When DH was<10 %, L431 also accorded with this hypothesis. However, the opposite result was presented in L431 when DH was>10 %.

The difference in the performance of L431 and LA-5 may be because the ability of *L. acidophilus* CEP is weak, which results in its low capacity to utilize macromolecular protein (Li et al., 2020). In addition, the ability of *L. acidophilus* to synthesize amino acids is minimal, and its nutritional requirement for amino acids is mainly satisfied by absorbing amino acids and oligopeptides in a growth medium (Azcarate-Peril et al., 2005). L431 had higher CEP activity than LA-5, and one of the representative CEPs, PrtP, was first identified in *L. paracasei* subsp. *paracasei* strains. The research on the utilization of nitrogen sources by *L. paracasei* is very limited, but Morishita et al. (1974) reported that its growth does not require amino acids such as Ala, Gly, His, Phe, and Pro. Previous studies have shown that the activity of CEP is not significantly affected by adding short peptides to growth media (Alcántara et al., 2016). In this study, its increment number was decreased after the addition of FGH-20, which may be due to the accumulation of a large number of peptides in the growing environment. Peptides catabolized by its own CEP and supplied by FGH-20 resulted in excessive peptide aggregation, inhibiting the expression of its protein hydrolysis system, and thus affecting its growth and proliferation. The proposed mechanism is shown in Fig. 1 (a-b).

3.2. Metabolic profiling of Lactobacillus by NMR and UPLC-MS

The dual platforms of NMR and UPLC-MS identified 92 and 112 metabolites in LA-5 and L431 (Tables S1-S4), respectively. Typical NMR spectra were shown in Figs. S2–S3. This result represented a significant improvement in the efficiency and coverage of metabolite detection compared to previous platforms that relied solely on NMR (44 metabolites) and UPLC-MS (47 significant metabolites) (Chen et al., 2022; Guo et al., 2022). For LA-5, in addition to 13 compounds (Glutamate, AMP, Phenylalanine, ADP, Xanthine, UMP, Tryptophan, Glutamine, PEP, Lactate, Aspartic Acid, Betaine, and Proline) that were detected in both NMR and LCMS, 16 and 25 were unique metabolites detected under ESI + and ESI- respectively, and 34 were detected only by NMR. For L431, except for 6 compounds, glutamic acid, UMP, glutamine, proline, choline, and lysine were identified by both methods. UPLC-MS ESI + and ESI- detected 31 and 35 unique metabolites respectively, while NMR detected 30 specific metabolites. This result showed that the two platforms have an excellent complementary effect. ^{1}H NMR has proved to be a gold technique for studying non-targeted metabolomics, which could effectively detect primary metabolites such as sugars, amino acids, organic acids, and nucleotides (Wang, Zhou, & Yang, 2022). However, due to the relatively low abundance of secondary metabolites such as

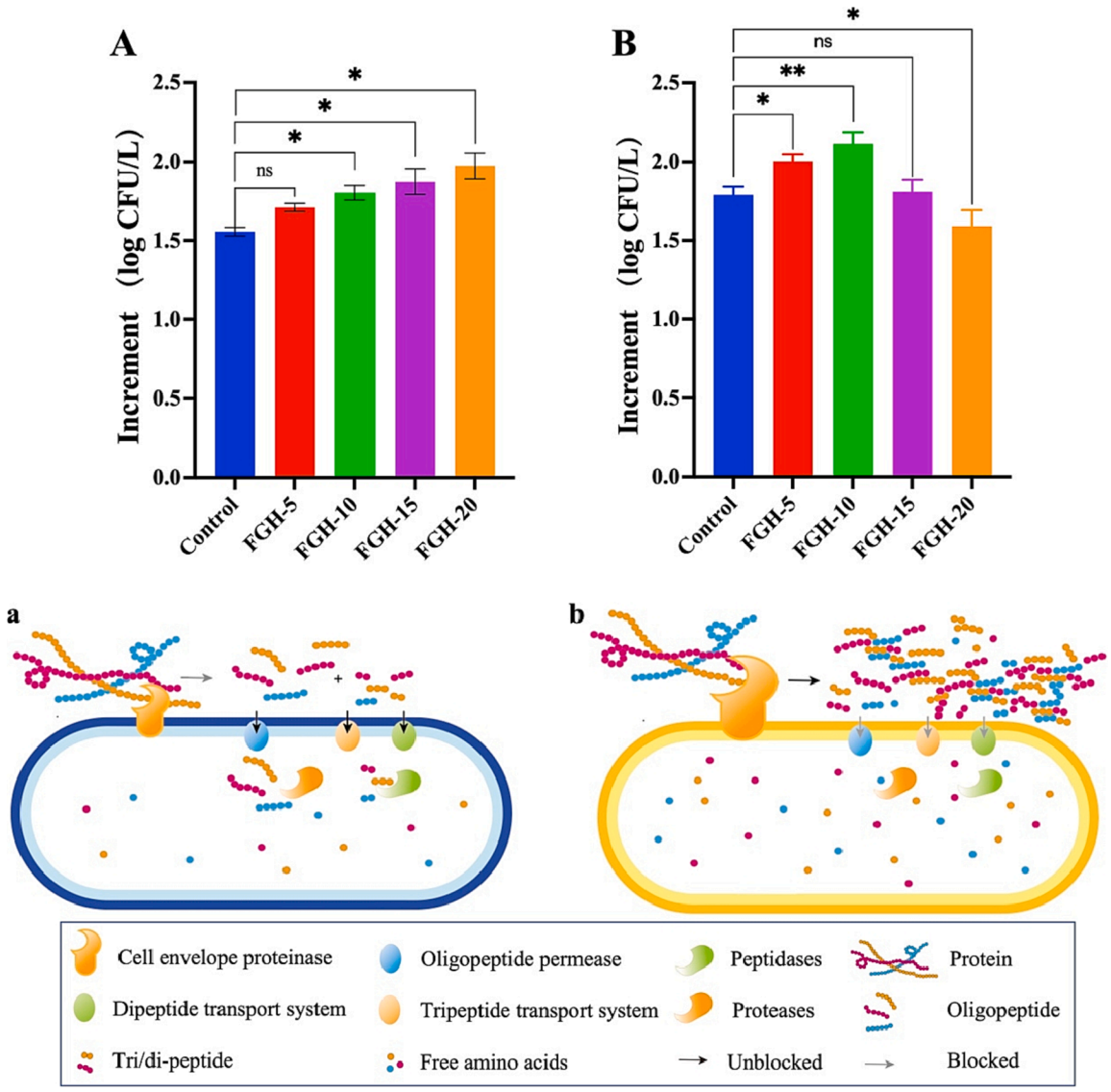

Fig. 1. Increment of probiotic cells (A: LA-5; B: L431) after adding different DH of FGH before and after fermentation and hypothetical mechanism of action on LA-5 (a) and L431 (b) after the addition of FGH. Data are expressed as mean ± standard deviation (n = 3). One-way ANOVA was applied to examine statistical significance between conditions, *: $P < 0.05$, **: $P < 0.01$, ns: no significant differences.

phenolic acids, flavonoids, and alkaloids, NMR quantitative detection is also quite tricky. LC-MS could supplement this part by being more sensitive than NMR, which enables the detection of metabolites with lower relative concentrations (Moco et al., 2008). Overall, the composition categories of probiotic metabolites detected from both platforms are presented in Fig. 2. It could be seen that although the two bacteria were different in species, the composition of the metabolite species was not notably significantly different, nucleotide-related compounds and amino acids accounted for almost half of all metabolites detected, and organic acids, sugars, lipids, and other substances accounted for the other half.

3.3. *Identification of metabolic differences in Lactobacillus in response to different DH of FGH*

In order to provide a global overview of metabolic profile and screen the main discriminative metabolites, PCA models based on the NMR, ESI + and ESI- datasets were conducted. In the NMR model of LA-5, the first three components accounted for a total of 73.12 % changes, PC1: 46.13 %, PC2: 16.25 %, and PC3: 10.74 %, respectively. The quality parameters of Q^2 and R^2X (Fig. 3) were 0.48 (above 0.45) and 0.73 (above 0.5), respectively, indicating that the predictability and interpretation of the model are satisfactory (Nurani et al., 2021). As for that of L431, the first three PCs accounted for the 75.78 % difference change, (PC1:39.5 %, PC2: 20.23 %, and PC3: 16.05 %). Q^2 was 0.586, and R^2X was 0.76. From the PCA diagram, it could be seen that the control group and the experimental group of L431 and LA-5 were obviously distinguished, which indicated that the metabolism of probiotics was affected by the hydrolysis of fish gelatin. There were significant differences for probiotics in metabolic states before and after the hydrolysis of FGH.

Based on the results of UPLC-MS ESI- and ESI+, four models were constructed with quality parameters shown in Table S5. R^2X being close to 1 and $Q^2 > 0.5$. The response parameters validated the quality of the models. The obvious distinction between the control group and the experimental group can be seen from the PCA score plot, which was similar to the results observed in NMR-based model. These results jointly revealed differences in the metabolic levels of probiotics before and after FG hydrolysis and further suggested that non-targeted metabolomics based on NMR and UPLC-MS might be a potential tool to identify specific biomarkers under different treatments.

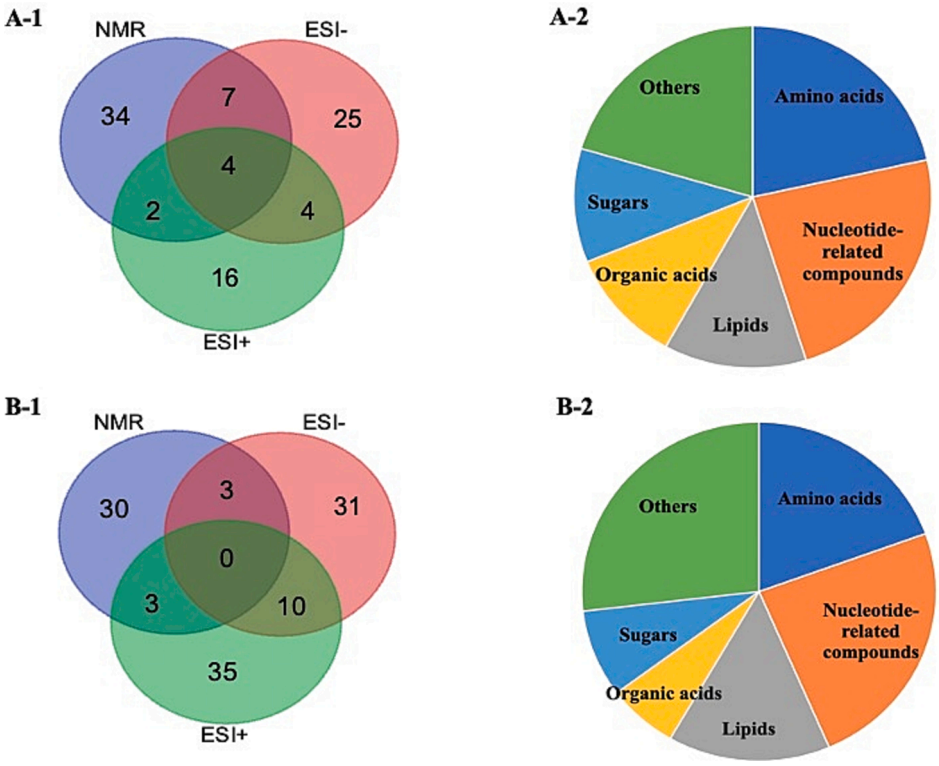

Fig. 2. Venn diagram showing the overlap of metabolites detected by NMR and UPLC-MS of LA-5 (A-1) and L431(B-1); metabolite composition of LA-5 (A-2) and L431 (B-2).

3.4. Altered metabolites in Lactobacillus by different DH of FGH

To clarify the detailed metabolic changes induced by different DH in *Lactobacillus*, the metabolites with significant changes after adding FGH were identified by OPLS-DA model. According to the results of influence of FGH with different DH on bacterial growth in Section 3.1, the FGH-10 and FGH-20 were chosen because of the obvious metabolic differences to establish OPLS-DA model by comparing with the control group. The data fitted well with OPLS-DA model (R^2Y: 0.985–0.991; Q^2: 0.899–0.988). OPLS-DA loading S-plots were provided based on the covariance *P* and correlation p(corr) between metabolites and modeled class designation. The dots below and above the X-axis represent lower and higher concentrations compared to their control sample (Fig. 4). Metabolites with VIP > 1 (colored in red) that made credible contributions were located at the far left or right side of the Fig. 4 to the separation of the paired samples. According to the *P* values, it can be further screened to be able to diagnose the metabolites with significant differences among treatments. Data from both platforms are summarized in Fig. 5.

For example, 24 of the metabolites such as Thr, Ala, Pro, Gln, GSH, ADP and AMP increased, and 13 of the metabolites such as Glu, NAD, UMP, PE decreased in abundance in the LA-5 (Fig. 5A) in response to FGH addition. As similar as LA-5, when FGH addition, 22 up-regulated components such as ADP, AMP, Xanthine and 9 down-regulated metabolites including NAD, Tyr, Choline in L431 (Fig. 5B) were found to be responsible for the differentiation with the control group. The metabolic response of probiotics to external treatment has been evaluated and significant perturbations in branched amino acids, and adenine were observed. Despite shared metabolic components, the response of different strains to such stress differed. These results indicated that variations in the differential metabolites may be responsible for the different reactions and alterations among probiotics to FGH. In addition, based on these differential variants, a hypothetical schematic diagram showing the main perturbations of LA-5 and L431 under FGH of different DH was presented in Fig. 6 to facilitate the future industrialization of probiotic fermented milk.

3.5. Metabolic network modulations in LA-5 after FGH addition

It has been proved that FGH can promote the growth of lactic acid bacteria. For LA-5, with the increase of DH, its efficiency for the proliferation of LA-5 also increases. However, its mechanism for promoting the growth of probiotics is still unclear. Here, FGH-10 and FGH-20 compared with FGH-0 were selected to analyze the metabolic pathway. The results showed that the majority of metabolic activities in LA-5 was related to the metabolism of amino acids, nucleotides, lipids and carbohydrates (Fig. 6).

3.5.1. Amino acid metabolism

In this experiment, the increases of all amino acids except glutamate were observed (Fig. 5A), indicating that the addition of FGH complemented the peptides and amino acids needed by LA-5 during its growth and promoted its amino acid metabolism. Some studies have found that under environmental changes, microorganisms respond to altered conditions by altering amino acid content in the cells (Chen et al., 2022). In this experiment, the addition of FGH created an ideal living environment for LA-5. Amino acids like Thr, Ala, Pro, GSH, Gln, Arg, Asp, Lys and Met all showed an up-regulation trend, which also indicated that the addition of FGH promoted the amino acid metabolism of LA-5. In addition, in Fig. 5A, it was observed that the FC values of FGH-20 were greater than that of FGH-10, indicating that FGH-20 had a more significant effect on amino acid metabolism changes than FGH-10. This result was also consistent with the increase of LA-5 in Section 3.1.

Among all the increased amino acids, arginine showed the most significant change in content, which might be because arginine played a crucial role in cell growth as well as early proliferation as a polyamine in the arginine and proline metabolic pathway, which regulates cell growth and differentiation, and modulates ion channels (Lefèvre et al.,

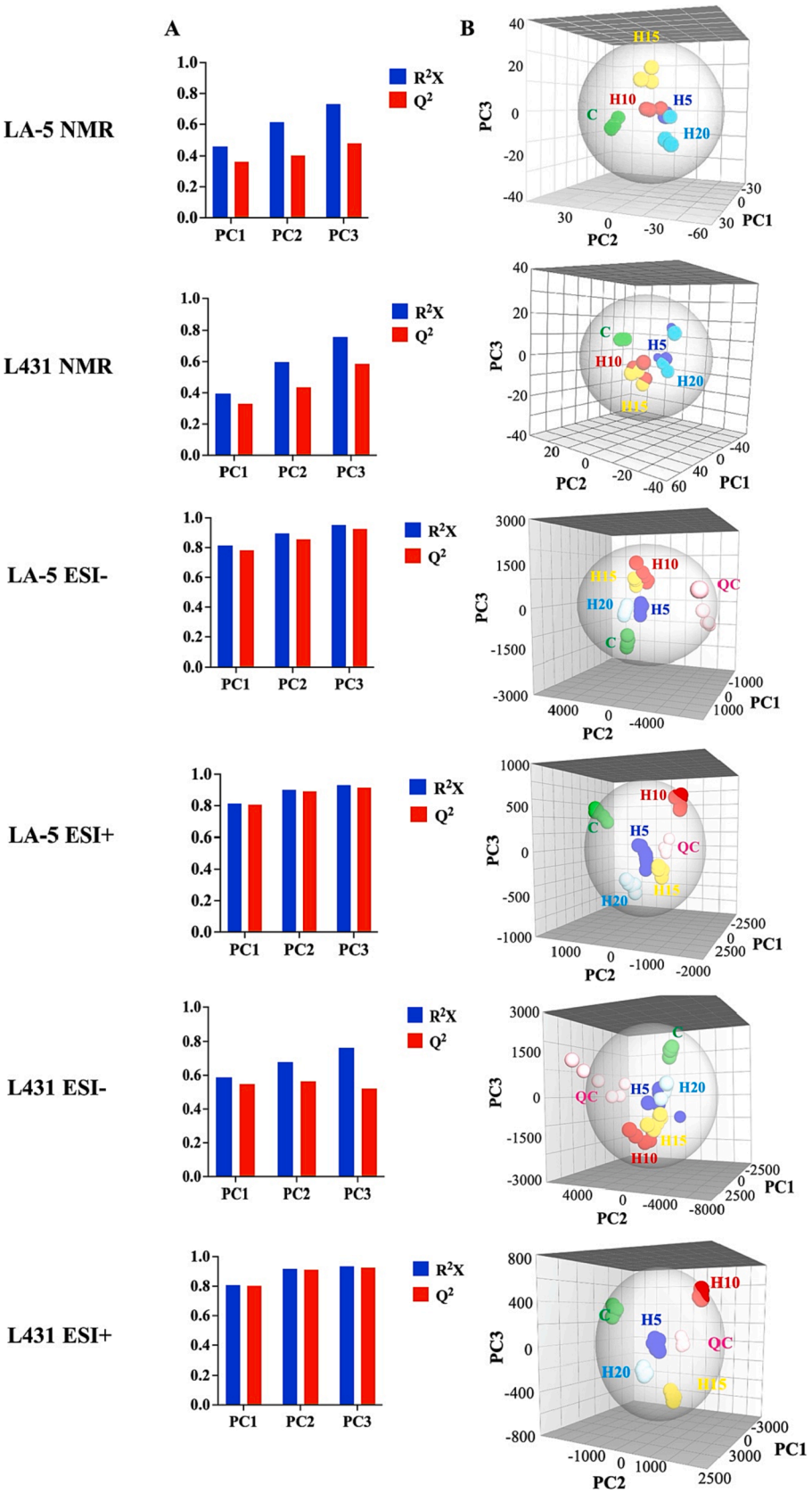

Fig. 3. Principal component analysis (PCA) of ^{1}H NMR and UPLC-MS spectra of *Lactobacillus*. Principal components explaining for the variances (A); score plot (B).

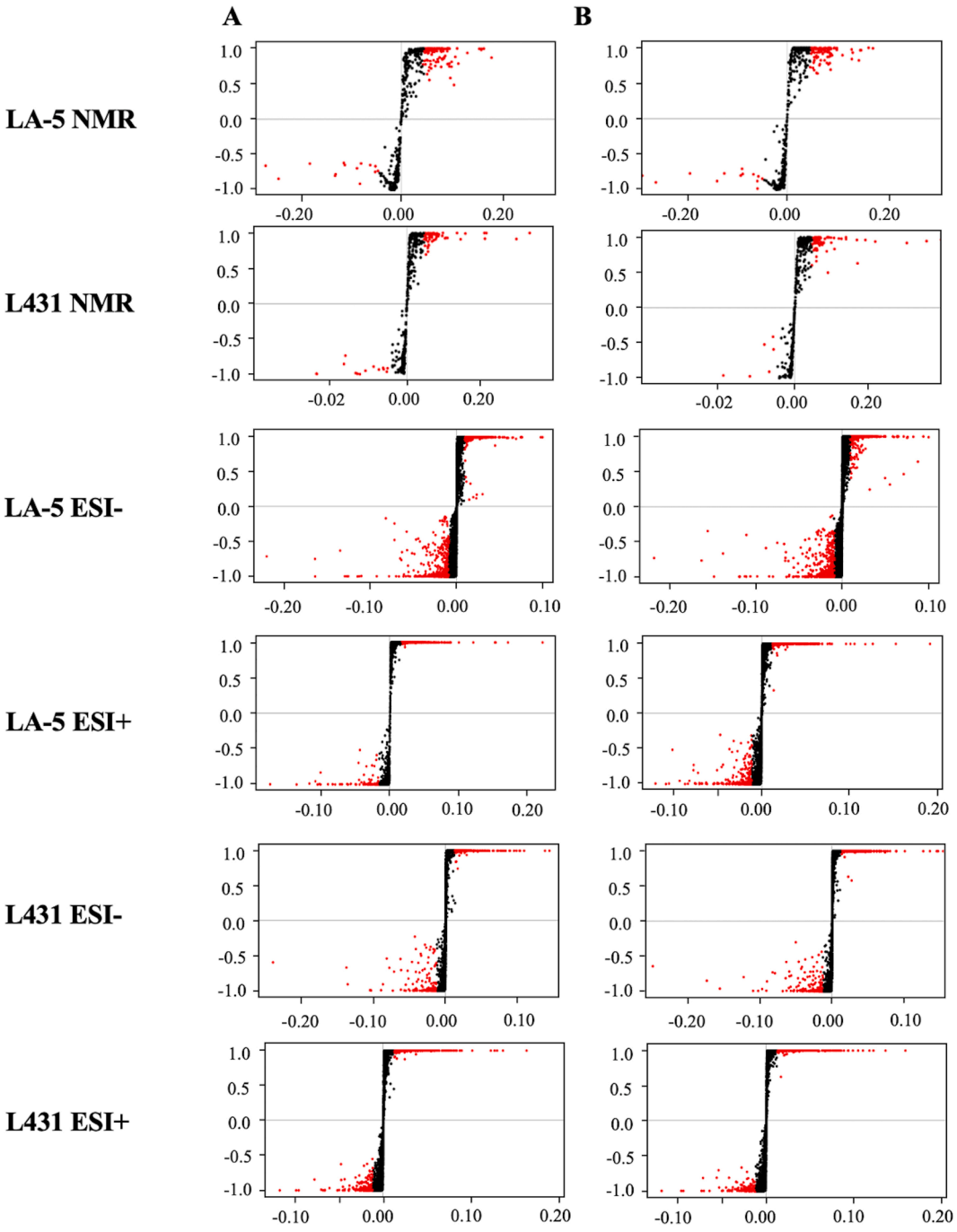

Fig. 4. Orthogonal partial least squares discriminant analysis (OPLS-DA) S-plots of NMR and UPLC-MS analysis of LA-5 and L431 strains. A: control vs FGH-10, B: control vs FGH-20.

2011). In addition, alanine, a glucogenic amino acid, can be converted to glucose for energy production through gluconeogenesis and glycolysis (Shi et al., 2022). It was differentially expressed in the experimental groups (a substantial increase was observed in the FGH-20 group), perhaps indicating that bacterial growth and proliferation were regulated by increasing energy supply. The decline in glutamate is also thought to be related to the addition of complex nitrogen sources. In previous studies, glutamic dehydrogenase was inhibited when a nitrogen source was added to the growth medium of the bacteria, and inhibited glutamate synthesis (Gunka & Commichau, 2012). Another possible reason is that glutamate often acts as an osmoprotectant, accumulating in response to adverse effects in the environment when cells are exposed to stress from the environment (Bearson et al., 2009). The decrease in glutamate content may further explain the supplementation of FGH with nutrients required for LA-5 growth and proliferation, providing an ideal growth environment for LA-5.

3.5.2. *Lipid metabolism*

In LA-5, significant changes in lipid content were also observed (Fig. 5A), and changes in lipids are usually associated with stress responses in cell membranes. Phosphatidylglycerol (PG) and phosphatidylethanolamine (PE) are the predominant cell membrane components that contribute to the structural stability and fluidity of the membrane (Bharatiya et al., 2021). Gram-positive bacteria can modulate their membrane composition at different growth stages and in different growth media to adjust the net charge in response to changes (Parsons &

A

	Metabolites	Detection means	C vs 10		C vs 20	
			FC	Trend	FC	Trend
Amino acid metabolism						
	Threonine	NMR	2.37	↑****	3.47	↑****
	Alanine	NMR	6.82	↑*	11.44	↑****
	Proline	NMR	2.47	↑*	2.96	↑**
	Glutamine	NMR	6.51	↑**	8.36	↑***
	Glutathione	NMR	4.10	↑**	5.72	↑****
	Arginine	NMR	26.68	↑**	39.24	↑***
	Aspartic acid	NMR	2.94	↑*	3.89	↑***
	Lysine	NMR			2.96	↑**
	Methionine	NMR			7.82	↑**
	Glutamate	ESI-	2.64	↓**	3.13	↓**
Lipid metabolism						
	PG(16:0/0:0)	ESI-	2.92	↓**	4.26	↓**
	PE(18:1/0:0)	ESI-	3.78	↓**	2.54	↓**
	PE(18:0/0:0)	ESI+	8.46	↓**	7.11	↓**
	PE(16:0/0:0)	ESI+	13.8	↓**	9.1	↓**
	Eicosapentaenoic Acid	ESI+	3.95	↑**	7.27	↑**
	PE(18:1/0:0)	ESI+	5.56	↓**	2.65	↓**
	LysoPC(20:0)	ESI+			3.35	↑**
	PE(17:1/0:0)	ESI+			4.41	↓**
Nucleotide metabolism						
	NADH	ESI-	10.8	↓**	37	↓**
	ADP	ESI-	3.35	↑**	2.96	↑**
	UDP	ESI-	2.94	↑**	3.04	↑**
	NAD	ESI-	2.08	↓**	2.2	↓**
	UMP	ESI-	2.13	↓**		
	NAD	ESI+	2.59	↓**	2.3	↓**
	AMP	ESI+	2.31	↑**	3.4	↑**
Glucose metabolism						
	Lactate	ESI-	3.12	↑**		
	Propylene glycol	NMR	4.32	↑*		
	Ethanol	NMR	1.92	↑*	2.47	↑****
	Mannitol	NMR	1.74	↑*	2.41	↑****
	β-glucose	NMR	2.71	↑**	3.09	↑**
	Glycerate	NMR	3.15	↑*	4.29	↑***
	Glyceraldehyde	NMR			1.79	↑****
Others						
	Pantethine	ESI-	23	↑**	31.2	↑**
	Pyroglutamic acid	NMR			6.62	↑**
	Acetylcholine	ESI+			2.98	↓**
	PhenylLactate	ESI-	6.61	↑**	5.8	↑**
	Carnitine	ESI+	5	↓**		

B

	Metabolites	Detection means	C vs 10		C vs 20	
			FC	Trend	FC	Trend
Nucleotide metabolism						
	Xanthine	ESI-	36.9	↑**	58	↑**
	Xanthine	ESI+	32.7	↑**	52.6	↑**
	UMP	ESI-	10.1	↑**	16.6	↑**
	UDP	ESI-	6.69	↑**	8.42	↑**
	GMP (guanosine monophc	ESI-	25.2	↑**	34.5	↑**
	Guanidylic acid/guanosine	ESI+	22.7	↑**	34.3	↑**
	ADP	ESI-	3.77	↑**	3.75	↑**
	FMN	ESI+	2.14	↑**	2.26	↑**
	FMN	ESI-	2.23	↑**	2.27	↑**
	AMP	ESI-	5.73	↑**	5.84	↑**
	NADH	ESI-	50.5	↓**	18.4	↓**
	NADP+	ESI-	4.32	↑**		
	3'-AMP (Adenosine 3'-mo	ESI+	28.1	↑**	32.5	↑**
	FAD	ESI+	2.52	↑**	2.18	↑**
	dGDP	ESI+	3.41	↑**	3.59	↑**
	cyclic ADP-ribose (cyclic	ESI+	2.19	↓**	3.08	↓**
	Hypoxanthine	ESI+	252	↑**	225	↑**
	NAD	ESI+			2.15	↓**
	Uracil	ESI+			244	↑**
	Cyclic AMP	NMR	4.39	↑*	41.86	↑****
Glucose metabolism						
	Glyceraldehyde	NMR			4.35	↑*
	Lactate	NMR	0.36	↓***		
	α-Glucose	ESI-	6.43	↑**		
Amino acids metabolism						
	Tyrosine	ESI-	2.03	↓**		
	Choline	ESI+	2.09	↓**	2.47	↓**
	Threonine	NMR	0.66	↓**		
Lipid metabolism						
	PG(16:0/18:1)	ESI-			3.11	↓**
	PS(13:0/0:0)	ESI+	30	↑**	21.7	↑**
	PC(14:0/0:0)	ESI+	632	↑**	587	↑**
	LysoPC(20:0)	ESI+			3.22	↑**
Others						
	PhenylLactate	ESI-	3.95	↑**		
	Carnitine	ESI+	19.8	↓**	27.5	↓**

Fig. 5. Differential metabolites in LA-5 (A) and L431 (B) from control vs FGH-10, control vs FGH-20 detected by NMR and UPLC-Q/TOF-MS.

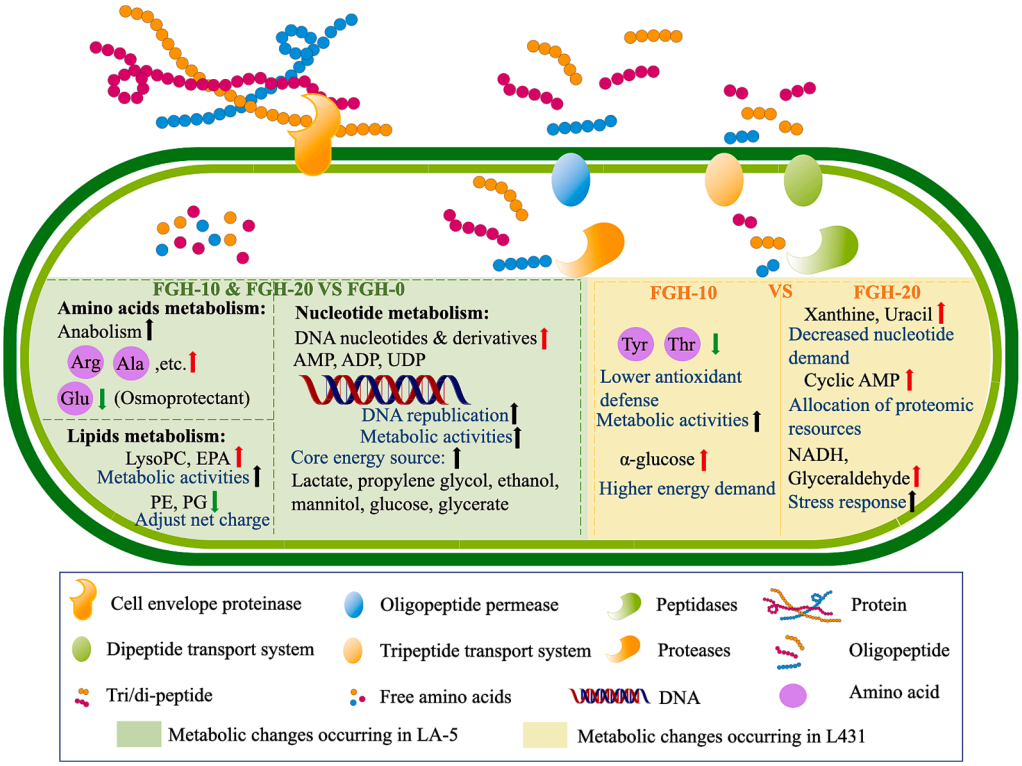

Fig. 6. Proposed schematic diagram of metabolic alterations.

Rock, 2013). In addition, membrane lipids were found to be involved in bacterial growth, and Lyso-PC could be used as a growth substrate for *Salmonella*, which consumes Lyso-PC to counteract the unfavorable host environment when nutritionally deficient (Antunes et al., 2011). This could explain why the Lyso-PC content in the bacterium increased instead after the addition of FGH. Eicosapentaenoic Acid (EPA) has been shown to be associated with the strength of cell membranes, and EPA also resists oxidative stress, so when EPA levels rise, the metabolic state of bacteria is also better (Nishida et al., 2006).

3.5.3. Nucleotide metabolism

A decrease in NAD and NADH was observed inside the cells (Fig. 5A), as a ubiquitous coenzyme, both involved in redox reactions of hundreds of enzymes (Dong et al., 2014), and the decrease in their content may indicate that the bacterial proliferation reached a steady state, completing the transition from the exponential to the stationary growth phase. UMP also showed a decrease after FGH addition. In previous studies, UMP synthesis resulted in more carbon metabolism in the pentose phosphate pathway, thereby inhibiting the fluxes of glycolysis and TCA cycle, both of which are closely related to bacterial energy supply and growth (Chen et al., 2010). The rise in UMP indicates high energy demand and good growth status of LA-5. In addition, an increase in adenine-related metabolites (AMP, ADP), pyrimidine nucleotides UDP was observed, and since these nucleotides are synthesized during DNA replication, cell growth, their increase could also indicate high energy demand and metabolic activities of the cells (Wang, Gao, et al., 2022). With this rise in demand, the metabolism of glucose, the source of LA-5 core competence, also rose, as evidenced by the rise in the content of Lactate, propylene glycol, ethanol, mannitol, glucose and glycerate in the strain (Jain et al., 2015).

3.6. Metabolic network modulations of L431 after FGH addition with different DH

The vast majority of metabolites observed to be significantly different in L431 (Fig. 5B, Fig. 6) after adding FGH were nucleotide-based, probably because most of the compounds detected by UPLC-MS were of the nucleotide-related compounds (Wang, Gao, et al., 2022). It is also possible that changes in environmental nitrogen caused significant perturbations to the nucleotide metabolism of L431. For example, Fitzsimmons et al. (2018) demonstrated its significant effect on nucleotide metabolism when nitrogen was starved. In addition, unlike LA-5, the addition of FGH significantly increased L431 cell growth at a DH of 10 %, while its growth decreased significantly at a DH of 20 %. To elucidate the mechanism of regulation of L431 metabolism by the degree of hydrolysis, the differences in metabolite expression between FGH-10 and FGH-20 were synthesized to elucidate the effect of the degree of hydrolysis on the amount of probiotic growth.

In the comparison of FGH-10 and FGH-20 groups with the control group, the difference in the fold change of the majority of metabolites was not significant, except for Xanthine. It was detected in both ESI- and ESI + modes and the data showed consistency in both modes. A substantial increase in the variation was also observed in FGH-20 compared to the increase in FGH-10. This may be because when hydrolysis is excessive, the increased small peptide and amino acid composition of the environment inhibits the expression of protease and thus the proliferation. L431 proliferation is retarded indicating a decrease in its nucleotide requirement (Bhat et al., 2015), subsequently, its degradation by purines would produce higher levels of Xanthine. In addition, a lesser reduction in NADH (reduction form of NAD) content was also observed in FGH-20 compared to FGH-10. The elevation of NADH is often associated with counteracting the stress response (Burns et al., 2010), which further supports that as the degree of hydrolysis increases, it is detrimental for the uptake and utilization with L431. Cyclic AMP, which ensures that proteomic resources are used in different metabolic sectors according to the needs of different nutritional environments (You et al., 2013), had significantly higher concentrations in FGH-20. This result is also consistent with previous findings that it accumulates intracellularly during nitrogen starvation (Hood et al., 1979).

A decrease in Tyrosine and Threonine was observed only in the FGH-

10 group, both metabolites associated with osmotic regulators, whose levels rise during their antioxidant defense (Zhang et al., 2021). In addition, a substantial rise in uracil was observed only in the FGH-20 group, and since uracil is present only in RNA, the changes suggest a facilitation of RNA synthesis, possibly because L431 is required to maintain proteins and enzymes necessary for cellular life activities when peptide uptake is blocked. Glyceraldehyde was elevated only in FGH-20, which is a highly reactive compound that crosslinks proteins and whose modified proteins appear to be cytotoxic, inhibiting intracellular glutathione levels and inducing ROS production, which adversely affects cells (Dharmaraja, 2017). And compared to FGH-20, there was an increase in α-Glucose content in FGH-10, indicating a rise in its glucose-related metabolism, and further indicating a better growth state and higher energy requirement in FGH-10 than in the FGH-20 group.

4. Conclusion

The effectiveness of FGH in promoting the growth of *Lactobacillus* was demonstrated in this work. The dual platform metabolomics study revealed that amino acid metabolism, lipid metabolism, and nucleotide metabolism pathways were key to the growth-promoting mechanism. Furthermore, when over-hydrolyzed FGH inhibited L431 growth, probiotics counteracted this adverse response by regulating nucleotide requirements, allocating protein resources, and adapting to adopt stress strategies. Overall, this study provided valuable insights into the probiotic growth-promoting mechanisms of FGH, and this finding may also serve as a scientific basis for the application of functional fermented dairy products with hydrolysate addition.

CRediT authorship contribution statement

Yi Le: Conceptualization, Methodology, Investigation, Software, Visualization, Writing – original draft, Writing – review & editing. **Xiaowei Lou:** Writing – original draft, Writing – review & editing. **Chengwei Yu:** Writing – original draft. **Chenxi Guo:** Visualization. **Yun He:** Software. **Yuyun Lu:** Software. **Hongshun Yang:** Resources, Writing – review & editing, Supervision, Project administration, Funding acquisition.

Declaration of Competing Interest

The authors declare that they have no known competing financial interests or personal relationships that could have appeared to influence the work reported in this paper.

Data availability

Data will be made available on request.

Appendix A. Supplementary data

Supplementary data to this article can be found online at https://doi.org/10.1016/j.foodchem.2022.135232.

References

Alcántara, C., Bäuerl, C., Revilla-Guarinos, A., Pérez-Martínez, G., Monedero, V., & Zúñiga, M. (2016). Peptide and amino acid metabolism is controlled by an OmpR-family response regulator in *Lactobacillus casei*. *Molecular Microbiology, 100*(1), 25–41.

Alemán, A., Giménez, B., Pérez-Santin, E., Gómez-Guillén, M., & Montero, P. (2011). Contribution of Leu and Hyp residues to antioxidant and ACE-inhibitory activities of peptide sequences isolated from squid gelatin hydrolysate. *Food Chemistry, 125*(2), 334–341.

Antunes, L. C. M., Andersen, S. K., Menendez, A., Arena, E. T., Han, J., Ferreira, R. B., … Finlay, B. B. (2011). Metabolomics reveals phospholipids as important nutrient sources during Salmonella growth in bile in vitro and in vivo. *Journal of Bacteriology, 193*(18), 4719–4725.

Ashraf, S. A., Nazir, S., Adnan, M., & Azad, Z. R. A. A. (2020). UPLC-MS: An emerging novel technology and its application in food safety. In *Analytical Chemistry-Advancement, Perspectives and Applications*. IntechOpen London.

Azcarate-Peril, M. A., McAuliffe, O., Altermann, E., Lick, S., Russell, W. M., & Klaenhammer, T. R. (2005). Microarray analysis of a two-component regulatory system involved in acid resistance and proteolytic activity in *Lactobacillus acidophilus*. *Applied and Environmental Microbiology, 71*(10), 5794–5804.

Bearson, B. L., Lee, I. S., & Casey, T. A. (2009). Escherichia coli O157: H7 glutamate-and arginine-dependent acid-resistance systems protect against oxidative stress during extreme acid challenge. *Microbiology, 155*(3), 805–812.

Benjakul, S., & Morrissey, M. T. (1997). Protein hydrolysates from Pacific whiting solid wastes. *Journal of Agricultural and Food Chemistry, 45*(9), 3423–3430.

Bharatiya, B., Wang, G., Rogers, S. E., Pedersen, J. S., Mann, S., & Briscoe, W. H. (2021). Mixed liposomes containing gram-positive bacteria lipids: Lipoteichoic acid (LTA) induced structural changes. *Colloids and Surfaces B: Biointerfaces, 199*, Article 111551.

Bhat, S. V., Booth, S. C., Vantomme, E. A., Afroj, S., Yost, C. K., & Dahms, T. E. (2015). Oxidative stress and metabolic perturbations in *Escherichia coli* exposed to sublethal levels of 2, 4-dichlorophenoxyacetic acid. *Chemosphere, 135*, 453–461.

Burns, P., Sánchez, B., Vinderola, G., Ruas-Madiedo, P., Ruiz, L., Margolles, A., … Clara, G. (2010). Inside the adaptation process of *Lactobacillus delbrueckii subsp. lactis* to bile. *International Journal of Food Microbiology, 142*(1–2), 132–141.

Chen, L., Zhao, X., Li, R., & Yang, H. (2022). Integrated metabolomics and transcriptomics reveal the adaptive responses of *Salmonella enterica* serovar Typhimurium to thyme and cinnamon oils. *Food Research International, 157*, Article 111241.

Chen, P., Chen, X., Yu, W., Zhou, B., Liu, L., Yang, Y., … Li, C. (2022). Ciprofloxacin stress changes key enzymes and intracellular metabolites of *Lactobacillus plantarum* DNZ-4. *Food Science and Human Wellness, 11*(2), 332–340.

Chen, Y., Li, S., Xiong, J., Li, Z., Bai, J., Zhang, L., … Ying, H. (2010). The mechanisms of citrate on regulating the distribution of carbon flux in the biosynthesis of uridine 5′-monophosphate by *Saccharomyces cerevisiae*. *Applied Microbiology and Biotechnology, 86*(1), 75–81.

Corona-Hernandez, R. I., Álvarez-Parrilla, E., Lizardi-Mendoza, J., Islas-Rubio, A. R., de la Rosa, L. A., & Wall-Medrano, A. (2013). Structural stability and viability of microencapsulated probiotic bacteria: A review. *Comprehensive Reviews in Food Science and Food Safety, 12*(6), 614–628.

Dharmaraja, A. T. (2017). Role of reactive oxygen species (ROS) in therapeutics and drug resistance in cancer and bacteria. *Journal of Medicinal Chemistry, 60*(8), 3221–3240.

Dong, W.-R., Sun, C.-C., Zhu, G., Hu, S.-H., Xiang, L.-X., & Shao, J.-Z. (2014). New function for *Escherichia coli* xanthosine phophorylase (xapA): Genetic and biochemical evidences on its participation in NAD+ salvage from nicotinamide. *BMC Microbiology, 14*(1), 1–10.

Emwas, A.-H. M. (2015). The strengths and weaknesses of NMR spectroscopy and mass spectrometry with particular focus on metabolomics research. *Metabonomics* (pp. 161-193).

Faraki, A., Noori, N., Gandomi, H., Banuree, S. A. H., & Rahmani, F. (2020). Effect of Auricularia auricula aqueous extract on survival of *Lactobacillus acidophilus* La-5 and *Bifidobacterium bifidum* Bb-12 and on sensorial and functional properties of synbiotic yogurt. *Food Science & Nutrition, 8*(2), 1254–1263.

Fitzsimmons, L. F., Liu, L., Kim, J.-S., Jones-Carson, J., & Vázquez-Torres, A. (2018). *Salmonella* reprograms nucleotide metabolism in its adaptation to nitrosative stress. *MBio, 9*(1), e00211-00218.

Gunka, K., & Commichau, F. M. (2012). Control of glutamate homeostasis in *Bacillus subtilis*: A complex interplay between ammonium assimilation, glutamate biosynthesis and degradation. *Molecular Microbiology, 85*(2), 213–224.

Guo, C., He, Y., Wang, Y., & Yang, H. (2022). NMR-based metabolomic investigation on antimicrobial mechanism of *Salmonella* on cucumber slices treated with organic acids. *Food Control, 137*, Article 108973.

Hood, E. E., Armour, S., Ownby, J. D., Handa, A. K., & Bressan, R. A. (1979). Effect of nitrogen starvation on the level of adenosine 3′, 5′-monophosphate in *Anabaena variabilis*. *Biochimica et Biophysica Acta (BBA)-General Subjects, 588*(2), 193–200.

Jain, R., Sun, X., Yuan, Q., & Yan, Y. (2015). Systematically engineering *Escherichia coli* for enhanced production of 1, 2-propanediol and 1-propanol. *ACS Synthetic Biology, 4*(6), 746–756.

Jung, S., Rickert, D., Deak, N., Aldin, E., Recknor, J., Johnson, L., & Murphy, P. (2003). Comparison of Kjeldahl and Dumas methods for determining protein contents of soybean products. *Journal of the American Oil Chemists' Society, 80*(12), 1169–1173.

Lazzi, C., Meli, F., Lambertini, F., Bottesini, C., Nikolaev, I., Gatti, M., … Neviani, E. (2013). Growth promotion of *Bifidobacterium* and *Lactobacillus* species by proteinaceous hydrolysates derived from poultry processing leftovers. *International Journal of Food Science & Technology, 48*(2), 341–349.

Lefèvre, P. L., Palin, M.-F., & Murphy, B. D. (2011). Polyamines on the reproductive landscape. *Endocrine Reviews, 32*(5), 694–712.

Li, W., Zhang, Y., Li, H., Zhang, C., Zhang, J., Uddin, J., & Liu, X. (2020). Effect of soybean oligopeptide on the growth and metabolism of Lactobacillus acidophilus JCM 1132. *RSC Advances, 10*(28), 16737–16748.

Moco, S., Forshed, J., De Vos, R. C., Bino, R. J., & Vervoort, J. (2008). Intra-and inter-metabolite correlation spectroscopy of tomato metabolomics data obtained by liquid chromatography-mass spectrometry and nuclear magnetic resonance. *Metabolomics, 4*(3), 202–215.

Morishita, T., Fukada, T., Shirota, M., & Yura, T. (1974). Genetic basis of nutritional requirements in *Lactobacillus casei*. *Journal of Bacteriology, 120*(3), 1078–1084.

Nishida, T., Orikasa, Y., Watanabe, K., & Okuyama, H. (2006). The cell membrane-shielding function of eicosapentaenoic acid for *Escherichia coli* against exogenously added hydrogen peroxide. *FEBS Letters, 580*(28–29), 6690–6694.

Nurani, L. H., Rohman, A., Windarsih, A., Guntarti, A., Riswanto, F. D. O., Lukitaningsih, E., … Rafi, M. (2021). Metabolite Fingerprinting Using ^{1}H-NMR Spectroscopy and Chemometrics for Classification of Three Curcuma Species from Different Origins. *Molecules, 26*(24), 7626.

Ozturkoglu-Budak, S., Akal, H. C., Buran, İ., & Yetişemiyen, A. (2019). Effect of inulin polymerization degree on various properties of synbiotic fermented milk including *Lactobacillus acidophilus* La-5 and *Bifidobacterium animalis* Bb-12. *Journal of Dairy Science, 102*(8), 6901–6913.

Parsons, J. B., & Rock, C. O. (2013). Bacterial lipids: Metabolism and membrane homeostasis. *Progress in Lipid Research, 52*(3), 249–276.

Shi, J., Xia, C., Tian, Q., Zeng, X., Wu, Z., Guo, Y., & Pan, D. (2022). Untargeted metabolomics based on LC–MS to elucidate the mechanism underlying nitrite degradation by *Limosilactobacillus fermentum* RC4. *LWT, 163*, Article 113414.

Wang, Y., Gao, X., & Yang, H. (2022). Integrated metabolomics of "big six" *Escherichia coli* on pea sprouts to organic acid treatments. *Food Research International, 111354*.

Wang, Y., Zhou, D., & Yang, H. (2022). Metabolic Responses of "Big Six" *Escherichia coli* in Wheat Flour to Thermal Treatment Revealed by Nuclear Magnetic Resonance Spectroscopy. *Applied and Environmental Microbiology, 88*(7), e00098–e122.

Yin, M., Yang, D., Lai, S., & Yang, H. (2021). Rheological properties of xanthan-modified fish gelatin and its potential to replace mammalian gelatin in low-fat stirred yogurt. *LWT, 147*, Article 111643.

You, C., Okano, H., Hui, S., Zhang, Z., Kim, M., Gunderson, C. W., … Hwa, T. (2013). Coordination of bacterial proteome with metabolism by cyclic AMP signalling. *Nature, 500*(7462), 301–306.

Zhang, H., Liu, J., Wen, R., Chen, Q., & Kong, B. (2021). Metabolomics profiling reveals defense strategies of *Pediococcus pentosaceus* R1 isolated from Harbin dry sausages under oxidative stress. *LWT, 135*, Article 110041.